RSC
Chemical Biology

ROYAL SOCIETY
OF **CHEMISTRY**

PAPER
Teruyuki Komatsu *et al.*
Haemoglobin(βK120C)–albumin trimer as an artificial O$_2$
carrier with sufficient haemoglobin allostery

PAPER

Haemoglobin(βK120C)–albumin trimer as an artificial O_2 carrier with sufficient haemoglobin allostery†

Yoshitsugu Morita, [ID] Asuka Saito, Jun Yamaguchi and Teruyuki Komatsu [ID] *

The allosteric O_2 release of haemoglobin (Hb) allows for efficient O_2 delivery from the lungs to the tissues. However, allostery is weakened in Hb-based O_2 carriers because the chemical modifications of the Lys- and Cys-β93 residues prevent the quaternary transition of Hb. In this paper, we describe the synthesis and O_2 binding properties of a recombinant Hb [rHb(βK120C)]–albumin heterotrimer that maintains sufficient Hb allostery. The rHb(βK120C) core, with two additional cysteine residues at the symmetrical positions on its protein surface, was expressed using yeast cells. The mutations did not influence either the O_2 binding characteristics or the quaternary transition of Hb. Maleimide-activated human serum albumins (HSAs) were coupled with rHb(βK120C) at the two Cys-β120 positions, yielding the rHb(βK120C)–HSA₂ trimer, in which the Cys-β93 residues were unreacted. Molecular dynamics simulation demonstrated that the HSA moiety does not interact with the amino acid residues around the haem pockets and the $α_1β_2$ surfaces of the rHb(βK120C) core, the alteration of which retards Hb allostery. Circular dichroism spectroscopy demonstrated that the quaternary transition between the relaxed (R) state and the tense (T) state of the Hb core occurred upon both the association and dissociation of O_2. In phosphate-buffered saline solution (pH 7.4) at 37 °C, the rHb(βK120C)–HSA₂ trimer exhibited a sigmoidal O_2 equilibrium curve with the O_2 affinity and cooperativity identical to those of native Hb (p_{50} = 12 Torr, n = 2.4). Moreover, we observed an equal Bohr effect and 2,3-diphosphoglycerate response in the rHb(βK120C)–HSA₂ trimer compared with naked Hb.

Introduction

Allosteric regulation plays a crucial role in controlling the protein function in biological systems through the binding of a small-molecule effector that induces a conformational change. Haemoglobin (Hb) is a well-known allosteric protein encapsulated in red blood cells (RBCs),[1–5] and its allostery has been extensively studied to understand its mechanism.[6–12] O_2 binding converts the quaternary structure of Hb from a deoxy tense (T) state with a low O_2 affinity to a relaxed (R) state with a high O_2 affinity.[1–4] The homotropic allosteric effect, which is known as cooperativity, allows Hb to efficiently transport O_2 from the lungs to the peripheral tissues. As a heterotropic allosteric effect, 2,3-diphospoglycerate (DPG) stabilizes the T-state conformation by creating salt bridges between the two β subunits to reduce O_2 affinity.[13,14] Furthermore, O_2 affinity

*Department of Applied Chemistry, Faculty of Science and Engineering,
Chuo University, 1-13-27 Kasuga, Bunkyo-ku, Tokyo 112-8551, Japan.
E-mail: komatsu@kc.chuo-u.ac.jp*

† Electronic supplementary information (ESI) available. See DOI: 10.1039/d0cb00056f
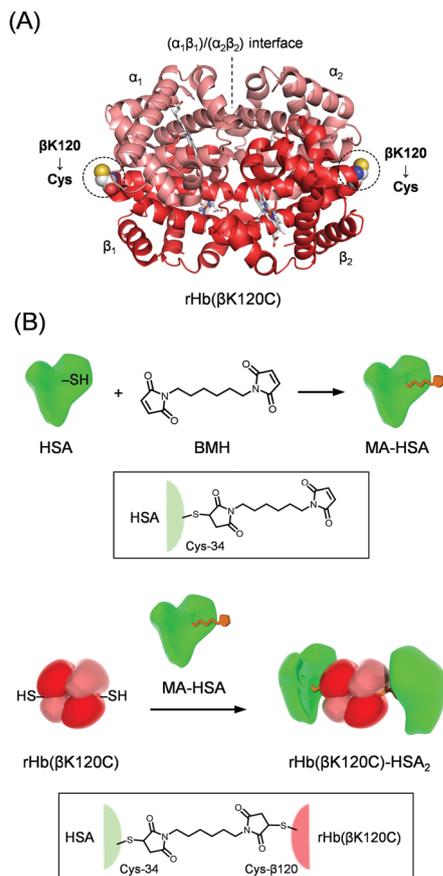
decreases with decreasing pH (the Bohr effect), shifting the equilibrium toward the T state.[11,15,16]

Artificial O_2 carriers are currently required as RBC substitutes for transfusion therapy because of worldwide shortages in blood supply.[17,18] However, the stroma-free Hb splits to an αβ dimer ($α_2β_2 → 2αβ$) in the bloodstream and is immediately expelled into urine. Moreover, Hb diffuses into the interstitial spaces between the endothelial cells and smooth muscle cells, causing hypertension by scavenging nitric oxide (NO; endothelial-derived vasodilator).[19,20] Therefore, naked Hb is not available for use in transfusion therapy. Since the 1980s, several types of Hb-based O_2 carriers have been developed, including cross-linked Hb,[21,22] polymerized Hb,[23,24] and PEGylated Hb.[25–27] However, these chemical modifications have markedly reduced cooperativity, the Bohr effect, and the DPG effect,[18] and a modified Hb that maintains the original allosteric effects of Hb has never been reported.[18] We previously synthesized a protein cluster as an RBC substitute consisting of an Hb molecule wrapped covalently in human serum albumins (HSAs), called an Hb–HSA$_m$ cluster (m = 2–4, average m = 3.0 ± 0.2).[28,29] This protein cluster shows a long circulation lifetime in the bloodstream and a superior biocompatibility.[30,31] The

Fig. 1 (A) Recombinant Hb variant [rHb(βK120C)] with Lys-β120 residues replaced by cysteines at the symmetrical positions. The mutation point was designed to avoid the haem pockets and $\alpha_1\beta_2$ interfaces. (B) Synthetic routes of maleimide-activated HSA (MA-HSA) and the rHb(βK120C)–HSA$_2$ trimer. The Cys-34 of the HSA was reacted with 1,6-bis(maleimido)hexane (BMH), resulting in MA-HSA. The two Cys-β120 residues at symmetrical positions were reacted with MA-HSA to yield the rHb(βK120C)–HSA$_2$ trimer.

quaternary structural analysis of the Hb–HSA$_m$ cluster revealed that the chemical modification of the Lys and Cys-β93 residues of Hb by N-succinimidyl 3-maleimidopropionate as a cross-linker prevents the R–T quaternary transition and maintains the Hb core close to the R state.[32] Thus, the Hb–HSA$_m$ cluster demonstrated a low cooperativity, a low Bohr effect, and a low DPG effect. If the HSA shells are linked at appropriate positions on the Hb surface so that they do not affect the R–T quaternary motion, the resulting Hb–HSA$_m$ conjugate maintains the original O$_2$ binding properties of the native Hb. The genetically introduced cysteine could act as a cross-linking point for maleimide-activated HSA (MA-HSA). We assume that the mutation of Hb residues, excluding the mutation of (i) the $\alpha_1\beta_2$ interfaces, including the N- and C-terminals (which play important roles in the R–T quaternary transition), and (ii) the haem pockets (which directly affect O$_2$ affinity), would allow the resulting Hb variant to maintain its original O$_2$ binding capability. Based on this hypothesis, the Lys-β120 residues were chosen as the symmetrical mutation points (Fig. 1A). In this study, we describe a novel recombinant Hb variant, rHb(βK120C), in which

Lys-β120 is replaced with Cys at symmetrical positions on the Hb surface, and we also present the rHb(βK120C)–HSA$_2$ hetero-trimer, in which MA-HSAs are linked at the Cys-β120 positions (Fig. 1B). Ultraviolet-Visible (UV-vis) and circular dichroism (CD) spectroscopies revealed that the quaternary structure of the rHb(βK120C)–HSA$_2$ trimer is reversibly convertible between the R and T states. We also observed identical O$_2$ affinity and allosteric effects in the rHb(βK120C)–HSA$_2$ trimer compared with naked Hb.

Results and discussion

Expression and physicochemical properties of rHb(βK120C)

We first expressed rHb(βK120C) using *Pichia* yeast (*Pichia pastoris* GS115) according to our previous reports.[33,34] The expressed rHb(βK120C) was purified using cation- and anion-exchange chromatographies (CEC and AEC). The sodium dodecyl sulfate–polyacrylamide gel electrophoresis (SDS–PAGE) analysis of rHb(βK120C) depicted two clear bands corresponding to the α- and β-subunits (Fig. 2A). The α- and β-chain bands demonstrated near-identical mobility to those of native Hb. The matrix-assisted laser desorption/ionization-time of flight (MALDI-TOF) mass spectrum analysis of rHb(βK120C) exhibited molecular-related ion peaks at 15 122 and 15 841 Da. These were almost identical to the simulated masses of the amino acid sequences (15 127 Da for the α-chain and 15 842 Da for the β-chain), indicating that Lys-β120 was replaced with cysteine. The size-exclusion chromatography (SEC) chromatogram of rHb(βK120C) exhibited a peak with the same elution volume as that of native Hb, indicating that the tetramer $(\alpha_1\alpha_2\beta_1\beta_2)$ was formed in the rHb(βK120C) (Fig. 2B; elution volume = 1.9 mL). Fortunately, the oligomeric rHb(βK120C) species created *via* the disulfide bonds of Cys-β120 was not observed in the SEC chromatogram. The fact that rHb(βK120C) and native Hb had identical CD spectra (λ = 200–250 nm) indicates that their secondary structures were equivalent (Fig. 2C). The isoelectric point (pI) value of rHb(βK120C) was determined to be 6.8, which was slightly lower than that of native Hb (pI = 6.9) because the mutation (Lys-β120 → Cys) had negatively shifted the net surface charge (Fig. S1, ESI†). The results of the sulfhydryl group assay using 4,4′-dithiodipyridine (4,4′-DTP)[35] revealed the number of reactive sulfhydryl groups in rHb(βK120C) and native Hb as 4.0 and 2.0, respectively. This result strongly indicates that the two Lys-β120 residues of the β_1 and β_2 chains were replaced by Cys and that the introduced Cys-β120 residues were reactive with 4,4′-DTP, as they are located at the molecular surface of rHb(βK120C).

Preparation of the rHb(βK120C)–HSA$_2$ trimer

To prepare MA-HSA, we used 1,6-bis(maleimido)hexane (BMH) as the cross-linking agent. One of the two maleimide groups in BMH was reacted with the free sulfhydryl group of the Cys-34 in HSA (which is the only reduced-form of cysteine in HSA), yielding MA-HSA. The formation of the HSA dimer was not observed because of electrostatic repulsion between the negatively charged HSA surfaces present under our experimental conditions. The
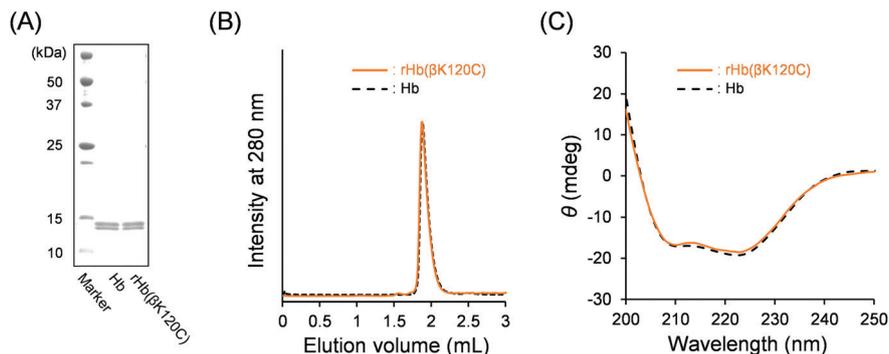
This journal is © The Royal Society of Chemistry 2020

RSC Chem. Biol., 2020, **1**, 128–136 | 129

Fig. 2 (A) SDS–PAGE results of native Hb and rHb(βK120C). (B) SEC profiles of rHb(βK120C) and native Hb. (C) CD spectra of the rHb(βK120C) and native Hb in PBS at 25 °C ([protein] = 0.2 μM).

sulfhydryl group assay using 4,4′-DTP revealed the complete disappearance of the reduced form.

Capping of the Cys-β93 residues of native Hb with maleimide derivatives causes a decline in O$_2$ binding cooperativity, the Bohr effect, and the influence of the allosteric effectors. The Cys-β93 residues of native Hb were able to react with maleimide derivatives, such as N-ethyl maleimide (NEM) and N-succinimidyl 3-maleimidopropionate.[32,36] We found that the Cys-β93 residues had not reacted with MA-HSA because of the steric hindrance between the native Hb and MA-HSA. In contrast, genetically introduced Cys-β120 located at the molecular surface of rHb(βK120C) had reacted with MA-HSA. The SEC chromatogram of the reaction mixture [rHb(βK120C) + MA-HSA] revealed a new peak in the high-molecular-weight region (Fig. 3A; elution volume = 1.4 mL), and native PAGE analysis also revealed

a new band above that of rHb(βK120C) (Fig. 3B). The high-molecular-weight component was purified using AEC followed by gel filtration chromatography (GFC). The ion peak of the β-chain at 15.8 kDa in the MALDI-TOF MS disappeared after the reaction of rHb(βK120C) with MA-HSA. A new peak then appeared at 82.5 kDa, a value almost identical to the simulated mass of a β-chain + MA-HSA (82.3 kDa), indicating that the HSA moiety was covalently linked to the β-chain of rHb(βK120C). Based on the [total protein]/[Hb unit] assays, the average HSA/Hb ratio of the product was determined to be 2.0. The heme loss was not observed during the preparation. We denoted this hybrid protein as rHb(βK120C)–HSA$_2$ (M_w: 198 kDa). The CD spectrum of the rHb(βK120C)–HSA$_2$ trimer coincided perfectly with the sum of the rHb(βK120C) spectrum and a two-times-enlarged HSA spectrum (Fig. 3C). This result demonstrates that the secondary structures

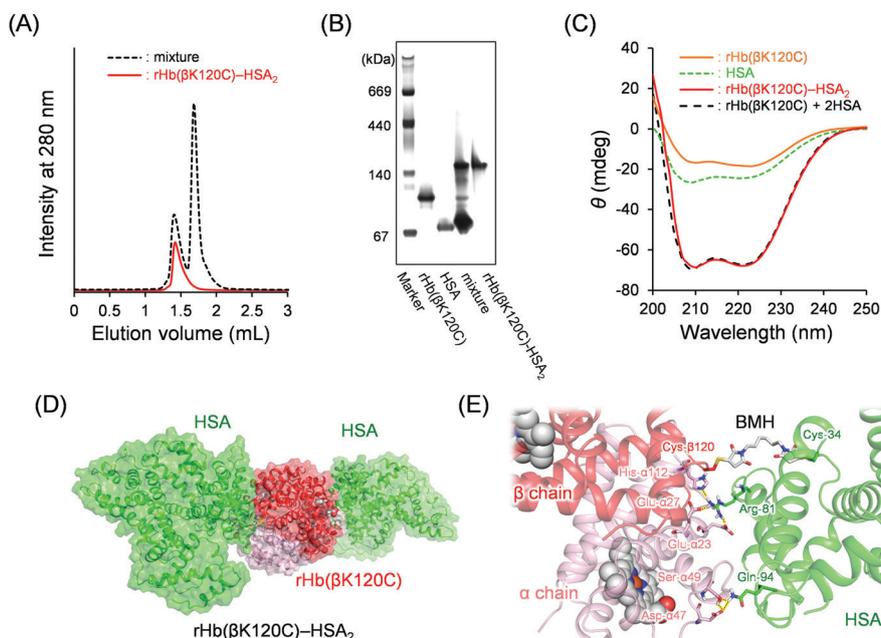**Fig. 3** (A) SEC profiles of the resultant reaction mixture [rHb(βK120C) + MA-HSA] and the purified rHb(βK120C)–HSA$_2$ trimer. (B) Native PAGE patterns of rHb(βK120C), HSA, the reaction mixture, and the purified rHb(βK120C)–HSA$_2$ trimer. (C) CD spectra of rHb(βK120C), HSA, rHb(βK120C), and rHb(βK120C)–HSA in PBS at 25 °C ([protein] = 0.2 μM). (D and E) The energy-minimized structure of the rHb(βK120C)–HSA$_2$ trimer obtained by a molecular dynamics (MD) calculation using the Desmond software.

130 | *RSC Chem. Biol.*, 2020, **1**, 128–136

This journal is © The Royal Society of Chemistry 2020

of the individual proteins were unaltered by the protein coupling. The dynamic light scattering measurements revealed that the hydro-dynamic diameter of the rHb(βK120C)–HSA₂ trimer (12.4 ± 2.8 nm, P.I. = 0.010) was significantly larger than that of rHb(βK120C) (6.9 nm ± 1.9 nm, P.I. = 0.004). The pI value of the trimer (pI = 5.4) was close to that of HSA (pI = 4.9), which further indicates the coupling of rHb(βK120C) (pI = 6.7) with HSAs (Fig. S1, ESI†). The net negative surface charge and the large molecular size could allow the rHb(βK120C)–HSA₂ trimer to circulate in the bloodstream for long periods of time and prevent the undesirable vasopressor response through NO depletion.[19,20] Furthermore, the sulfhydryl group assay using 4,4′-DTP[35] demonstrated that the number of reactive sulfhydryl groups in the rHb(βK120C)–HSA₂ trimer was 1.8, indicating that the Hb core maintained the free Cys-β93 residues that are important for O_2 binding ability, as mentioned above.[36] We could not observe the dissociation of the $\alpha_2\beta_2$ tetramer into two $\alpha\beta$ dimers during the synthesis, purification, and measurements of rHb(βK120C)–HSA₂, implying that the $\alpha_2\beta_2$ tetramer was sufficiently stable the same as native Hb under our experimental conditions.

An MD simulation was used to predict the interactions between the rHb(βK120C) and HSA moieties. The Cys-$\beta_1$120 and Cys-$\beta_2$120 residues exist at symmetrical positions of the core Hb; therefore, a sufficient distance is maintained between the two HSA parts in the rHb(βK120C)–HSA₂ trimer. We performed MD simulation using a half model [αβ(K120C)–HSA] constructed using the crystal structures of native Hb (PDB ID: 2DN1)[37] and HSA (PDB ID: 1AO6)[38] (Fig. S2, ESI†). The main chains (Cα and amide atoms) of the αβ(K120C) moiety were frozen for the duration of a 50 ns simulation. The root-mean-square deviation (RSMD) and the distances of the salt bridges and hydrogen bonds between the αβ(K120C) and HSA residues reached a plateau within 25 ns (Fig. S3, ESI†). The MD simulation structure was represented in the rHb(βK120C)–HSA₂ form which was prepared by overlapping the two αβ(K120C) moieties of the models with the crystal structure of native Hb ($\alpha_1\beta_1\alpha_2\beta_2$; Fig. 3D and Fig. S2B, ESI†). The distance between the sulfide atoms of Cys-β120 [rHb(βK120C)] and Cys-34 (HSA) was measured to be 13.8 Å, meaning that the BMH was long enough to cross-link the Cys residues (Fig. 3E). We found that the following salt bridges and hydrogen bonding interactions between rHb(βK120C) and HSA helped stabilize the conformation of the rHb(βK120C)–HSA₂ trimer: (i) Glu-α23, Glu-α27, and His-α112 of rHb(βK120C)—Arg-81 of HSA and (ii) Ser-α49 and Asp-α47 of rHb(βK120C)—Gln-94 of HSA. The HSA moiety did not interact with the amino acid residues around the haem pockets and the $\alpha_1\beta_2$ surfaces of the rHb(βK120C) core.

Quaternary structure analysis of the Hb core

We investigated the quaternary structure of the Hb core using UV-vis absorption and CD spectroscopies. The UV-vis spectral patterns and the absorbances of the oxy, deoxy, and carbonyl rHb(βK120C) as well as the rHb(βK120C)–HSA₂ trimer were indistinguishable from those of native Hb in PBS solution (pH 7.4; Fig. 4A and Table S1, ESI†). Generally, the chemical modification of the Lys and Cys-β93 residues of Hb decreases
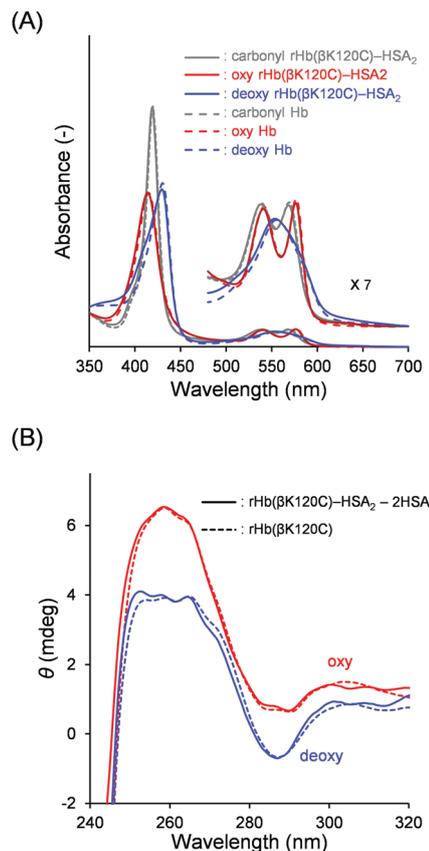

Fig. 4 (A) UV-vis absorption spectra of the carbonyl (gray), oxy (red), and deoxy (blue) rHb(βK120C)–HSA₂ trimer (solid line) and native Hb (dotted line). (B) CD spectra (240–320 nm) of the oxy (red) and deoxy (blue) Hb components of the rHb(βK120C)–HSA₂ trimer [rHb(βK120C)–HSA₂ − twofold HSA] (solid line) and rHb(βK120C) (dotted line). The measurements were performed in PBS solution (pH 7.4) at 25 °C ([protein] = 3 μM).

the Soret band absorption of the deoxy form, because the deoxy Hb remains near the R-state quaternary structure.[32] In contrast, the deoxy rHb(βK120C) and the rHb(βK120C)–HSA₂ trimer revealed the same Soret band absorption as that of deoxy native Hb, indicating that the identical T-state quaternary structures were formed. CD spectroscopy was also used to analyse the quaternary structure of the Hb core in the rHb(βK120C)–HSA₂ trimer. Generally, deoxy Hb (T state) exhibits a negative CD band at 287 nm, which is known as the T-state marker.[39–41] At the same time, this band is not usually observed in the R-state quaternary structure of oxy Hb. The CD spectral patterns and intensities of oxy and deoxy rHb(βK120C) both resembled those of native Hb, implying that the oxy and deoxy forms of these proteins are comparable (Fig. 4B).[39] CD also revealed similar spectral changes in the rHb(βK120C)–HSA₂ trimer upon deoxygenation. CD spectra for the oxy and deoxy Hb cores in the rHb(βK120C)–HSA₂ trimer were obtained by subtracting the two-times-enlarged HSA spectrum from the corresponding rHb(βK120C)–HSA₂ trimer spectra (Fig. 4B). The CD spectra of the oxy and deoxy Hb cores coincided with those of rHb(βK120C). These spectral analyses revealed that the mutation Lys-β120 → Cys and coupling of HSA at the Cys-β120 positions did

This journal is © The Royal Society of Chemistry 2020

RSC Chem. Biol., 2020, **1**, 128–136 | **131**

not influence the quaternary structural transition between the R and T states.

O$_2$ binding affinity and cooperativity

Hb binds with O$_2$ in the lungs, where there is a high O$_2$ partial pressure (pO_2), and releases O$_2$ into the peripheral tissues, where there is a low pO_2. To evaluate the O$_2$ binding properties, O$_2$ affinity (p_{50}; pO_2 where Hb is half-saturated with O$_2$) and the Hill coefficient (n; degree of cooperativity) of Hb were determined from the O$_2$ equilibrium curve (OEC). As shown in Fig. 5A, a sigmoidal OEC was observed for native Hb in PBS solution (pH 7.4) at 37 °C (p_{50} = 12 Torr; n = 2.4). Upon the release of O$_2$, the quaternary structure of Hb converts from the R state with a high O$_2$ affinity to the T state with a low O$_2$ affinity. The cooperative O$_2$ release allows Hb to efficiently deliver O$_2$ from the lungs to the tissues. Nevertheless, chemically

modified Hbs have demonstrated a low cooperativity because the quaternary transition of the Hb core is prevented.[32] Such modified Hbs include PEG-Hb (71% reduction),[18,42] polymerized Hb (41% reduction),[18,42] and Hb–HSA$_m$ clusters (71% reduction).[29,42] In contrast, the OECs of rHb(βK120C) and the rHb(βK120C)–HSA$_2$ trimer were found to have a sigmoidal shape completely consistent with that of native Hb (Fig. 5A). The O$_2$ binding parameters of rHb(βK120C) (p_{50} = 12 Torr, n = 2.3) and the rHb(βK120C)–HSA$_2$ trimer (p_{50} = 12 Torr, n = 2.4) were also equivalent to those of native Hb (Table 1). Both rHb(βK120C) and the rHb(βK120C)–HSA$_2$ trimer were able to maintain identical O$_2$ affinity and cooperativity because the quaternary structure of the Hb units was interconvertible between the R and T states upon O$_2$ association and dissociation, as in native Hb. The capping of Cys-β93 with NEM in native Hb (NEM-Hb) reduced the p_{50} and n values (p_{50} = 8 Torr, n = 1.9). The NEM-rHb(βK120C)–HSA$_2$ trimer demonstrated O$_2$ binding parameters similar to those of NEM-Hb, clearly indicating that the Cys-β93 residues in the rHb(βK120C)–HSA$_2$ trimer were in a reduced form. This result is supported by the sulfhydryl group assay mentioned above. We concluded that the selective coupling of MA-HSA occurred at the two Cys-β120 positions of the rHb(βK120C), whereas it did not take place at the Cys-β93 residues because of steric hindrance. On the basis of these findings, we also concluded that the Lys-β120 → Cys mutation and the selective conjugation of MA-HSA at the Cys-β120 positions were impervious to O$_2$ affinity and cooperativity. To the best of our knowledge, this is the first example of a chemically modified Hb showing an identical O$_2$ affinity and cooperativity to those of native Hb.[18]

The autoxidation rate constant (k_{ox}) of the oxygenated Hb core in the rHb(βK120C)–HSA$_2$ trimer was measured in PBS solution (pH 7.4) at 37 °C. The k_{ox} value of the rHb(βK120C)–HSA$_2$ trimer was ascertained as 0.027 h^{-1}, which was almost similar to the data of native Hb (0.020 h^{-1}). The oxy form of the internal Hb maintains good stability even after being covered with HSAs.

Bohr effect on rHb(βK120C)–HSA$_2$ trimer

A high metabolic activity leads to an increase in the concentration of CO$_2$ and a decrease in the pH value within the tissues. Under low-pH conditions, the protonation of Hb occurs and the T-state quaternary structure is stabilized, reducing O$_2$ affinity (the Bohr effect). Thus, the OEC of native Hb was right-shifted to a p_{50} value of 28 Torr at pH 6.2 compared with p_{50} = 12 Torr at
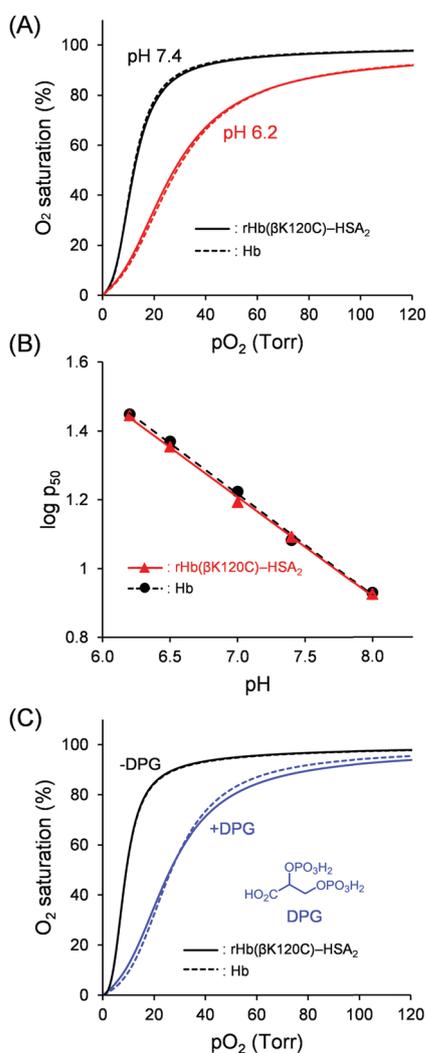

Fig. 5 OECs and Bohr plots of Hb (dotted line) and the rHb(βK120C)–HSA$_2$ trimer (solid line) at 37 °C ([protein] = 5 μM). (A) OECs in PBS solutions at pH 7.4 (black) and pH 6.2 (red). (B) The Bohr plots of Hb (black circle) and the rHb(βK120C)–HSA$_2$ trimer (red triangle) in PBS solutions (pH 6.2, 6.5, 7.0, 7.4, and 8.0). (C) OECs in 50 mM Tris–HCl buffer solution with 1 mM DPG (blue) and without DPG (black).

Table 1 O$_2$ binding parameters and Bohr coefficients of haemoproteins in PBS solution at 37 °C

| Haemoprotein | pH 7.4 | | pH 6.2 | | Bohr coefficient[a] |
	p_{50} (Torr)	n (—)	p_{50} (Torr)	n (—)	
Hb	12	2.4	28	1.9	0.29
rHb(βK120C)	12	2.3	29	1.9	0.29
rHb(βK120C)–HSA$_2$	12	2.4	28	1.9	0.29

[a] The Bohr coefficients were derived from the slopes obtained from plotting $-\Delta \log p_{50}/\Delta$pH between pH 6.2 and 8.0 (Fig. 5B).

132 | *RSC Chem. Biol.*, 2020, **1**, 128–136

This journal is © The Royal Society of Chemistry 2020

Table 2 Effect of DPG on hemoproteins in 50 mM Tris–HCl buffer solution (pH 7.4) at 37 °C containing 1 mM DPG

Hemoprotein	Without DPG		With DPG	
	p_{50} (Torr)	n (—)	p_{50} (Torr)	n (—)
Hb	9	2.3	27	2.4
rHb(βK120C)	9	2.3	26	2.1
rHb(βK120C)–HSA$_2$	9	2.3	26	2.1

pH 7.4 (Table 1 and Fig. 5A). The Bohr effect allows for Hb high O$_2$-transport efficiency to the tissues. However, chemical modifications have tended to notably reduce the Bohr effect, such as in PEG-Hb (87% reduction)[18] and polymerized Hb (75% reduction).[18] We observed that the O$_2$ affinities of rHb(βK120C) and the rHb(βK120C)–HSA$_2$ trimer were reduced under lower pH conditions, similar to native Hb (p_{50}: 12 → 29 Torr (pH 7.4 → 6.2)). The p_{50} and n values of both rHb(βK120C) and the rHb(βK120C)–HSA$_2$ trimer were nearly identical to those of native Hb at pH 6.2 (Table 1). The Bohr coefficients were derived from the slopes obtained from plotting $-\Delta\log p_{50}/\Delta\text{pH}$ between pH 6.2 and 8.0 (Fig. 5B and Table S2, ESI†). The Bohr coefficients of both rHb(βK120C) and the rHb(βK120C)–HSA$_2$ trimer were identical to those of native Hb (Table 1). The value measured for native Hb, however, was somewhat weaker than the result reported by Ho *et al.*[43] This difference is probably attributable to several factors, such as the difference in temperature (37 °C *vs.* 29 °C) and the difference in solvents (PBS with low phosphate and high NaCl concentrations *vs.* 0.1 M sodium phosphate buffer (PB)). Altogether, we conclude that neither the Lys-β120 → Cys mutation nor the HSA conjugation affected the Bohr effect.

Effects of DPG on O$_2$ binding affinity

Allosteric effectors bind to proteins, altering their activity. The most important allosteric regulator of Hb in RBCs is DPG, which reduces the O$_2$ binding affinity (the DPG effect). An X-ray crystallography analysis has previously revealed that a single DPG molecule binds to the cleft of Hb β chains, known as the DPG binding site.[13,14] The anionic groups of DPG form salt bridges with the cationic groups of the β-chains, including the His-β2, Lys-β82, and His-β143 residues, stabilizing the T-state conformation and reducing O$_2$ affinity. The T → R conformational change induced by oxygenation leads to the closure of the binding site and weakens the DPG binding affinity to oxy Hb. This DPG response allows Hb to efficiently deliver O$_2$ from the lungs to the tissues. We measured the OEC of native Hb in PBS (pH 7.4) solution containing 1 mM DPG at 37 °C, but a reduction in O$_2$ affinity was not observed because of the fact that phosphate anions in the PBS solution interrupt the binding of DPG to Hb. Thus, we used 0.1 M Tris–HCl buffer for DPG response experiments. Indeed, native Hb in Tris–HCl buffer demonstrated a higher O$_2$ affinity (p_{50} = 9 Torr) than in PBS solution because of the exclusion of the Hb–phosphate anion interactions (Table 2). The O$_2$ affinity of the native Hb was also reduced upon the addition of DPG to Tris–HCl buffer. Interestingly, rHb(βK120C) (p_{50} = 26 Torr) and the rHb(βK120C)–HSA$_2$ trimer (p_{50} = 26 Torr) demonstrated identical DPG responses to

native Hb (p_{50} = 27 Torr; Fig. 5C). These results indicate that the rHb(βK120C)–HSA$_2$ trimer maintained a DPG response similar to that of native Hb and that its O$_2$ affinity is controllable *via* the allosteric effector.

Conclusions

A novel Hb variant (Lys-β120 → Cys) was designed to prepare the rHb(βK120C)–HSA$_2$ trimer as an artificial O$_2$ carrier. The mutation did not affect the O$_2$ binding properties of Hb. Two MA-HSA molecules were selectively linked to Cys-β120 in rHb(βK120C), resulting in the rHb(βK120C)–HSA$_2$ trimer in which Cys-β93 remained free because of steric repulsion between the rHb(βK120C) core and the MA-HSA shell. The CD spectra revealed that the R–T quaternary motion of the Hb core in the rHb(βK120C)–HSA$_2$ trimer occurred upon O$_2$ association and dissociation. Thus, the rHb(βK120C)–HSA$_2$ trimer demonstrated sufficient allosteric O$_2$ binding properties with respect to cooperativity, the Bohr effect, and the DPG effect. The rHb(βK120C)–HSA$_2$ trimer is a unique artificial O$_2$ carrier with sufficient allostery to be an RBC substitute.

Materials and methods

Materials and apparatus

1,6-Bis(maleimido)hexane (BMH) was purchased from Tokyo Chemical Industry Co., Ltd. Human serum albumin (HSA, albumin 25%, Benesis) was purchased from the Japan Blood Products Organization. The other special-grade chemicals were used without additional purification unless otherwise noted. Water was deionized (18.2 MΩ cm) using two water purification systems (Elix UV and Milli Q Reference; Millipore Corp.). The SDS–PAGE and native PAGE analyses were performed using a 15% or 5–12% poly(acrylamide) precast gel (SuperSep Ace 15%; SuperSep Ace 5–12%; Fujifilm Wako Pure Chemical Corp.). Isoelectric focusing (IEF) was performed using a pH 3–10 IEF protein gel (Novex; Thermo Fischer Scientific Inc.). The UV-vis absorption spectra were obtained using a UV-Visible spectrophotometer (8543; Agilent Technologies Inc. or V-650; Jasco Corp.). CD spectra were recorded using a CD spectrometer (J-820; Jasco Corp.) at 25 °C.

Expression and preparation of rHb(βK120C)

The expression plasmid for the rHb(βK120C) variant [pHIL-D2-rHb(βK120C)] was constructed according to the standard protocol of the QuickChange XL Site-Directed Mutagenesis Kit (Agilent Technologies Inc.) using a pHIL-D2-rHb(α- and β-chains) vector[34] and an oligonucleotide primer set (forward [5′-CTCGCGCATCACTTCGGCT**GT**GAGTTTACACCGCCAGTTC-3′] and reverse [5′-GAACTGGCGGTGTAAACTCA**CA**GCCGAAGTGAT-GCGCGAG-3′]). The obtained pHIL-D2-rHb(βK120C) vector was linearized with *Sal*I and used to transform the GS115-strain *Pichia pastoris* (Thermo Fisher Scientific K.K.) *via* electroporation.

Transformed clone cells were grown in a buffered mineral glycerol complex (BMGY) medium (4 L total) in a shaking

This journal is © The Royal Society of Chemistry 2020

RSC Chem. Biol., 2020, **1**, 128–136 | 133

incubator (Bio-Shaker G·BR-200; Taitec Corp.; 200 rpm, 30 °C) and subsequently in a buffered mineral methanol complex (BMMY) medium (1.6 L total) containing 0.3 mM hemin for 5 days. During cultivation, 100% methanol at 1.5% of the medium volume was added every 24 h. The cells were harvested by centrifugation at 3000g for 10 min. The obtained cells were then washed with water (300 mL × 2) and resuspended in 100 mL of sodium PB solution (10 mM, pH 6.0) containing 1 mM phenylmethanesulfonyl fluoride. After the addition of glass beads (150 mL, d = 0.5 mm), the cells were lysed using a BeadBeater (Biospec Products, Inc.) with four cycles of disruption (2 min) and incubated by cooling on ice (2 min). After centrifugation at 12 000g for 1 h, the supernatant was equilibrated with CO atmosphere. The solution was loaded onto a cation exchange chromatography column (SP Sepharose Fast Flow, GE Healthcare UK Ltd), which was equilibrated in 10 mM PB (pH 6.0). After washing with the same buffer solution, the target protein was eluted using 20 mM Tris–HCl buffer solution (pH 8.0). Next, the resulting protein solution was subjected to AEC using a Q Sepharose Fast Flow column (GE Healthcare UK Ltd) with 20 mM Tris–HCl (pH 8.0) as the running buffer. After washing with 20 mM Tris–HCl (pH 8.0), rHb(βK120C) was eluted using PBS solution (pH 7.4). The purity was checked using SDS–PAGE analysis and SEC on a high-performance liquid chromatography (HPLC) system (AKTA purify; GE Healthcare UK Ltd). The system was equipped with an SEC column (Superdex 200 Increase, 5/150 GL; GE Healthcare UK Ltd), and PBS solution (pH 7.4) was used as the mobile phase. The concentration of rHb(βK120C) was measured using a protein assay kit (Pierce 660 nm; Thermo Fisher Scientific K.K.). The obtained rHb(βK120C) had a concentration of approximately 100 mg L^{-1} of media. The sulfhydryl group assay of rHb(βK120C) was conducted by reaction with 4,4′-dithiodipyridine (4,4′-DTP).[35]

Preparation of MA-HSA

The 25% HSA solution (4 mL) was diluted with PBS solution (14 mL, pH 7.4). A DMSO solution of BMH (7.5 mM, 2 mL) was then added dropwise to the HSA solution (8.4 mM, 18 mL). After stirring for 3 h at 25 °C, the reactant was subjected to a GFC column (Sephadex G25 superfine; GE Healthcare UK Ltd) to remove the unreacted cross-linker. The protein concentration was measured using a protein assay kit (Pierce 660 nm), whereas the sulfhydryl group assay of MA-HSA was conducted by reaction with 4,4′-DTP. The MA-HSA solution was stored at −80 °C.

Preparation of rHb(βK120C)–HSA₂

The MA-HSA and rHb(βK120C) solutions were mixed and concentrated to 6 mL ([MA-HSA] = 0.4 mM, [rHb(βK120C)] = 0.1 mM). The reactant was stirred under dark conditions for 24 h at 4 °C. An aliquot of the reaction mixture was analysed using SEC on an HPLC system (AKTA purify; GE Healthcare UK Ltd) equipped with an SEC column (Superdex 200 Increase, 5/150 GL; GE Healthcare UK Ltd) and using PBS solution (pH 7.4) as the mobile phase. The reaction mixture was purified using AEC using a Q Sepharose Fast Flow column (GE Healthcare UK Ltd). The mixture solution was diluted with the same volume of water

and loaded onto the column equilibrated with PBS solution. The column was then washed using 10 mM PB (pH 7.4) solution. The rHb(βK120C)–HSA₂ trimer was eluted with a 10 mM PB (pH 6.0) + 120 mM NaCl solution. Under this condition, the HSA dimer remained in the column. The collected solution was concentrated and subjected to GFC using a Superdex 200 pg column (GE Healthcare UK Ltd) to isolate the rHb(βK120C)–HSA₂ trimer (yield: 50%). The total protein and Hb concentrations were measured using a protein assay kit (Pierce 660 nm; Thermo Fischer Scientific Inc.) and the extinction coefficient of cyano-metHb (ε_{541} = 4.4 × 10^4 M^{-1} cm^{-1}), respectively. The average [HSA]/[rHb(βK120C) unit] ratio of the product was estimated to be 2.0. The sulfhydryl group assay of MA-HSA was conducted *via* the reaction with 4,4′-DTP.

Molecular dynamics simulations

MD simulations were performed using the Desmond application implemented in a Maestro graphical interface.[44,45] We used the optimized potentials for liquid simulations (OPLS_2005) force field implemented in the Desmond software for all molecules in the system.[46] We constructed a half model of rHb(βK120C) [αβ(K120C)–HSA model] because rHb(βK120C)–HSA₂ has a C_2 symmetry, and there has to be a sufficient distance between the HSAs for their interactions to be negligible. The crystal structure of native Hb (PDB ID: 2DN1)[37] was used for the αβ(K120C) model. Lys-β120 was replaced with Cys using the PyMOL software (PyMOL Molecular Graphics System Version 2.0, Schrödinger, LLC.). For the HSA moiety, we used the crystal structure of HSA (PDB ID: 1AO6).[38] The missing atoms of the side chains in the HSA were added to the model using the PyMOL software. The water molecules in the model were removed. The bond orders were assigned, and the hydrogen atoms were added to the models using the Protein Preparation Wizard tool[47] in the Maestro software. The αβ(K120C) and HSA models were covalently linked using the BMH cross-linker [Cys-β120(αβ)-BMH-Cys-34(HSA)] and arranged so that sufficient distance was maintained between them (Fig. S2A, ESI†). The Cys-β120(Hb), Cys-34(HSA), and BMH moieties were minimized using the 3D builder in the Maestro software. The hydrogen networks and the protonated states were optimized to pH 7 using the Protein Preparation Wizard for which the pK_a values of the protein residues were predicted using PROPKA.[48] The αβ(K120C)–HSA model was solvated using explicit TIP3P water[49] with a buffering distance of 10 Å in an octahedral box. Sodium counterions were added to neutralize the charges. The model was relaxed using a default relaxation protocol implemented in the Desmond software. An isothermal–isobaric MD simulation was performed for 50 ns to maintain the 300 K temperature and 1.01325 bar pressure. The main chains (Cα and amide atoms) of the αβ(K120C) moiety were frozen during the simulation. The time step was 2 fs, and the information for analysis was printed every 100 ps. A 10 Å cut off was used for non-bonded interactions.

Preparation of oxy and deoxy forms of the rHb(βK120C)–HSA₂ trimer

The oxy (O₂ complex) rHb(βK120C)–HSA₂ trimer solution (PBS, pH 7.4, 3 μM, 3 mL) was prepared using our previously reported

134 | *RSC Chem. Biol.,* 2020, **1**, 128–136

This journal is © The Royal Society of Chemistry 2020

technique.[29] The solution was transferred to an optical quartz cuvette (10 mm path length) with a rubber septum cap. N_2 gas was blown into the oxy-form solution to yield the deoxy rHb(βK120C)–HSA$_2$ trimer. The UV-vis absorption and CD spectra of these species were recorded at 25 °C.

O$_2$ binding parameters

The O$_2$ affinity (p_{50}; O$_2$ partial pressure where Hb is half-saturated with O$_2$) and Hill coefficient (n) were determined using an automatic recording system for the O$_2$ equilibrium curve (Hemox Analyzer; TCS Scientific Corp.) at 37 °C. The oxy-form of the rHb(βK120C)–HSA$_2$ trimer solution (PBS, pH 7.4, approximately 5 μM, 4 mL) was used for the measurements. The trimers in PBS solution (pH 7.4) were deoxygenated by flushing with N_2 and oxygenated by increasing the O$_2$ partial pressure.

O$_2$ complex stability

The oxy form stability of the rHb(βK120C)–HSA$_2$ trimer was assessed using the first-order autoxidation rate constant (k_{ox}) of the core Hb using our earlier described procedures.[50]

Conflicts of interest

There are no conflicts to declare.

Acknowledgements

Notes and references

1 M. F. Perutz, H. Muirhead, J. M. Cox and L. C. G. Goaman, *Nature*, 1968, **219**, 131–139.
2 M. F. Perutz, *Nature*, 1970, **228**, 726–734.
3 J. Baldwin and C. Chothia, *J. Mol. Biol.*, 1979, **129**, 175.
4 G. Fermi, M. F. Perutz, B. Shaanan and R. Fourme, *J. Mol. Biol.*, 1984, **175**, 159.
5 W. A. Eaton, E. R. Henry, J. Hofrichter and A. Mozzarelli, *Nat. Biol.*, 1999, **6**, 351–358.
6 S. Adachi, S. Y. Park, J. R. H. Tame, Y. Shiro and N. Shibayama, *Proc. Natl. Acad. Sci. U. S. A.*, 2003, **100**, 7039–7044.
7 E. M. Jones, G. Balakrishnan and T. G. Spiro, *J. Am. Chem. Soc.*, 2012, **134**, 3461–3471.
8 C. Viappiani, S. Abbruzzetti, L. Ronda, S. Bettati, E. R. Henry, A. Mozzarelli and W. A. Eaton, *Proc. Natl. Acad. Sci. U. S. A.*, 2014, **111**, 12758–12763.
9 N. Shibayama, K. Sugiyama, J. R. Tame and S. Y. Park, *J. Am. Chem. Soc.*, 2014, **136**, 5097–5105.
10 E. M. Jones, E. Monza, G. Balakrishnan, G. C. Blouin, P. J. Mak, Q. H. Zhu, J. R. Kincaid, V. Guallar and T. G. Spiro, *J. Am. Chem. Soc.*, 2014, **136**, 10325–10339.
11 Y. Yuan, M. F. Tam, V. Simplaceanu and C. Ho, *Chem. Rev.*, 2015, **115**, 1702–1724.
12 N. Shibayama, A. Sato-Tomita, M. Ohki, K. Ichiyanagi and S. Y. Parkc, *Proc. Natl. Acad. Sci. U. S. A.*, 2020, **117**, 4741–4748.
13 A. Arnone, *Nature*, 1972, **237**, 146–149.
14 V. Richard, G. G. Dodson and Y. Mauguen, *J. Mol. Biol.*, 1993, **233**, 270–274.
15 C. Ho and I. M. Russu, *Biochemistry*, 1987, **26**, 6299–6305.
16 T.-Y. Fang, M. Zou, V. Simplaceanu, N. T. Ho and C. Ho, *Biochemistry*, 1999, **38**, 13423–13432.
17 A. Mozzarelli, L. Ronda, S. Faggiano, S. Bettati and S. Bruno, *Blood Transfus.*, 2010, **8**, s59–s68.
18 F. Meng, T. Kassa, S. Jana, F. Wood, X. Zhang, Y. Jia, F. D'Agnillo and A. I. Alayash, *Bioconjugate Chem.*, 2018, **29**, 1560–1575.
19 S. C. Schultz, B. Grady, F. Cole, I. Hamilton and K. Burhop, *J. Lab. Clin. Med.*, 1993, **122**, 301–308.
20 D. H. Doherty, M. P. Doyle, S. R. Curry, R. J. Vali, T. J. Fattor, J. S. Olson and D. D. Lemon, *Nat. Biotechnol.*, 1998, **16**, 672–676.
21 R. Chatterjee, E. V. Welty, R. Y. Walder, S. L. Pruitt, P. H. Rogers, A. Arnone and J. A. Walder, *J. Biol. Chem.*, 1986, **261**, 9929–9937.
22 E. Nagababu, S. Ramasamy, J. M. Rifkind, Y. Jia and A. I. Alayash, *Biochemistry*, 2002, **41**, 7407–7415.
23 J. S. Jahr, M. Moallempour and J. C. Lim, *Expert Opin. Biol. Ther.*, 2008, **8**, 1425–1433.
24 R. Kluger, J. S. Foot and A. A. Vandersteen, *Chem. Commun.*, 2010, **46**, 1194–1202.
25 K. D. Vandegriff, A. Malavalli, J. Wooldridge, J. Lohman and R. M. Winslow, *Transfusion*, 2003, **43**, 509–516.
26 B. M. Manjula, A. Tsai, R. Upadhya, K. Perumalsamy, P. K. Smith, A. Malavalli, K. Vandegriff, R. M. Winslow, M. Intaglietta, M. Prabhakaran, J. M. Friedman and A. S. Acharya, *Bioconjugate Chem.*, 2003, **14**, 464–472.
27 D. Li, T. Hu, B. N. Manjula and S. A. Acharya, *Bioconjugate Chem.*, 2009, **20**, 2062–2070.
28 D. Tomita, T. Kimura, H. Hosaka, Y. Daijima, R. Haruki, K. Ludwig, C. Böttcher and T. Komatsu, *Biomacromolecules*, 2013, **14**, 1816–1825.
29 R. Funaki, T. Kashima, W. Okamoto, S. Sakata, Y. Morita, M. Sakata and T. Komatsu, *ACS Omega*, 2019, **4**, 3228–3233.
30 R. Haruki, T. Kimura, H. Iwasaki, K. Yamada, I. Kamiyama, M. Kohno, K. Taguchi, S. Nagao, T. Maruyama, M. Otagiri and T. Komatsu, *Sci. Rep.*, 2015, **5**, 12778.
31 H. Iwasaki, K. Yokomaku, M. Kureishi, K. Igarashi, R. Hashimoto, M. Kohno, M. Iwazaki, R. Haruki, M. Akiyama, K. Asai, K. Nakamura, R. Funaki, Y. Morita and T. Komatsu, *Artif. Cells, Nanomed., Biotechnol.*, 2018, **46**, S621–S629.
32 Y. Morita, T. Yamada, M. Kureishi, K. Kihira and T. Komatsu, *J. Phys. Chem. B*, 2018, **122**, 12031–12039.
33 Y. Morita, K. Igarashi, R. Funaki and T. Komatsu, *ChemBioChem*, 2019, **20**, 1684–1687.
34 R. Funaki, W. Okamoto, C. Endo, Y. Morita, K. Kihira and T. Komatsu, *J. Mater. Chem. B*, 2020, **8**, 1139–1145.

This journal is © The Royal Society of Chemistry 2020

RSC Chem. Biol., 2020, **1**, 128–136 | 135

35 D. R. Grassetti and J. F. Murry Jr., *Arch. Biochem. Biophys.*, 1967, **119**, 41–49.

36 Y. Cheng, T. J. Shen, V. Simplaceanu and C. Ho, *Biochemistry*, 2002, **41**, 11901–11913.

37 S. Y. Park, T. Yokoyama, N. Shibayama, Y. Shiro and J. R. Tame, *J. Mol. Biol.*, 2006, **360**, 690–701.

38 S. Sugio, A. Kashima, S. Mochizuki, M. Noda and K. Kobayashi, *Protein Eng.*, 1999, **12**, 439–446.

39 M. F. Perutz, J. E. Ladner, S. R. Simon and C. Ho, *Biochemistry*, 1974, **13**, 2163–2173.

40 Y. Aki-Jin, Y. Nagai, K. Imai and M. Nagai, in *New Approaches in Biomedical Spectroscopy*, ed. K. Kneipp, R. Aroca, H. Kneipp and E. Wentrup-Byrne, American Chemical Society, Washington, DC, 1st edn, 2007, ch. 19, vol. 963, pp. 297–311.

41 M. Nagai, S. Nagatomo, Y. Nagai, K. Ohkubo, K. Imai and T. Kitagawa, *Biochemistry*, 2012, **51**, 5932–5941.

42 The cooperativity reduction was determined using the following equation, cooperativity reduction $(\%) = (n_{\text{native Hb}} - n)/(n_{\text{native Hb}} - 1.0) \times 100$, where $n_{\text{native Hb}}$ and n are Hill coefficient of native Hb and chemically modified Hb, respectively, and are measured in the same conditions. When the cooperativity is completely lost, the Hill coefficient becomes 1.0 and the cooperativity reduction reaches 100%.

43 M. E. Wiltrout, J. L. Giovannelli, V. Simplaceanu, J. A. Lukin, N. T. Ho and C. Ho, *Biochemistry*, 2005, **44**, 7207–72017.

44 *Desmond Molecular Dynamics System*, D. E. Shaw Research, Maestro-Desmond Interoperability Tools, Schrödinger LLC, New York, NY, 2016.

45 *Maestro*, Schrödinger Release 2017-3, Schrödinger LLC, New York, NY, 2017.

46 J. L. Banks, H. S. Beard, Y. Cao, A. E. Cho, W. Damm, R. Farid, A. K. Felts, T. A. Halgren, D. T. Mainz, J. R. Maple, R. Murphy, D. M. Philipp, M. P. Repasky, L. Y. Zhang, B. J. Berne, R. A. Friesner, E. Gallicchio and R. M. Levy, *J. Comput. Chem.*, 2005, **26**, 1752–1780.

47 Schrödinger Suite 2012 *Protein Preparation Wizard*, LLC, New York, NY, 2012; *Impact version 5.8*, Schrödinger, LLC, New York, NY, 2012.

48 M. H. M. Olsson, C. R. Søndergard, M. Rostkowski and J. H. Jensen, *J. Chem. Theory Comput.*, 2011, **7**, 525–537.

49 W. L. Jorgensen, J. Chandrasekhar, J. D. Madura, R. W. Impey and M. L. Klein, *J. Chem. Phys.*, 1983, **79**, 926–935.

50 K. Yamada, K. Yokomaku, M. Kureishi, M. Akiyama, K. Kihira and T. Komatsu, *Sci. Rep.*, 2016, **6**, 36782.